Experimental report

11/02/2025

Proposal: **5-31-2815** **Council:** 10/2020

Title: Crystal and magnetic structure studies of SmFeTiO5-based antiferromagnetic materials

Research area: Materials

This proposal is a new proposal

Main proposer: **Juan Pablo BOLLETTA**

Experimental team: Gabriel Julio CUELLO
Emmanuelle SUARD
Juan Pablo BOLLETTA

Local contacts: Gabriel Julio CUELLO
Emmanuelle SUARD
Henry FISCHER

Samples: (152Sm)CrTiO5
SmFeTiO5
SmCr0.25Fe0.75TiO5
SmCr0.50Fe0.50TiO5
SmCr0.75Fe0.25TiO5
Sm0.90Y0.10FeTiO5
(152Sm)Cr0.50Fe0.50TiO5
SmCrTiO5

Instrument	Requested days	Allocated days	From	To
D2B	2	2	18/06/2021	20/06/2021
D4	6	2	16/06/2021	18/06/2021

Abstract:

Compounds with the RMn2O5 structure type have attracted attention due to reports of magnetoelectric and multiferroic properties. We have obtained the isostructural SmFe1-xCrxTiO5 materials (x = 0, 0.25, 0.50, 0.75, 1). Initial results indicate a rich, mainly antiferromagnetic behavior and magnetodielectricity at low temperatures. Transition metal cations are distributed between sites with octahedral and square pyramidal geometries. Interatomic distances from XRPD and Mössbauer spectroscopy results indicate that site distribution is changing across the series. It is our hypothesis that the differences observed in physical properties are strongly influenced by this distribution. Neutron powder diffraction will allow the observation and refinement of magnetic structures as well as reveal the distribution of transition metals, oxygen content and position, and M-O-M angles, all relevant for the interpretation of magnetic properties. Natural samarium is a strong absorbent of thermal neutrons, but this will be mitigated by the use of higher-energy neutrons and by the substitution of natural Sm by the Sm-152 isotope. We are proposing a combined study in instruments D4 and D2B.

Structural studies of SmFeTiO5-based antiferromagnetic materials

The results of this study are reported in
A. E. Susloparova, J. P. Bolletta, B.Kobzi, A. A. Paecklar, S. Jouen, F. Fauth, V. Nachbaur, V. Nassif, E. Suard, D. Sedmidubsky, A. I. Kurbakov, A. Maignan, and C. Martin,
Structural and magnetic properties of $SmCrTiO_5$,
Phys. Rev. B, 2024, **110**, 224429
DOI: 10.1103/PhysRevB.00.004400

In this paper, we used a multi technic approach: synchrotron X-ray powder diffraction, neutron powder diffraction, Mossbauer spectroscopy, magnetization vs temperature and magnetic field, AC-magnetic susceptibility and DFT calculations.
The figures that illustrate the publication are copied below.

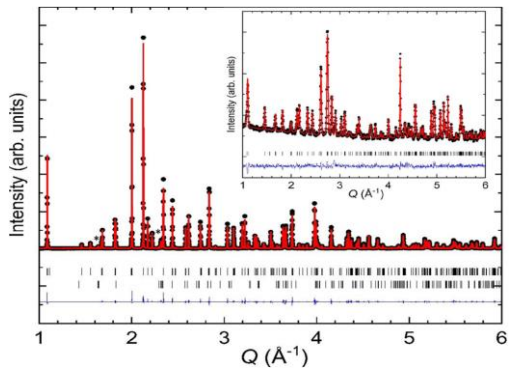

FIG. 1. Room-temperature SXRPD patterns of $SmCrTiO_5$: experimental, and calculated; difference patterns depicted as black circles, a red line and a blue line, respectively. The upper row of ticks corresponds to the Bragg reflections of the main *Pbam* phase and the lower one to an impurity (<1. 5% in mass) with an orthorhombic perovskite-type structure. The two most intense impurity peaks are indicated by asterisks (*). Inset: RT NPD patterns of ^{152}Sm $CrTiO_5$

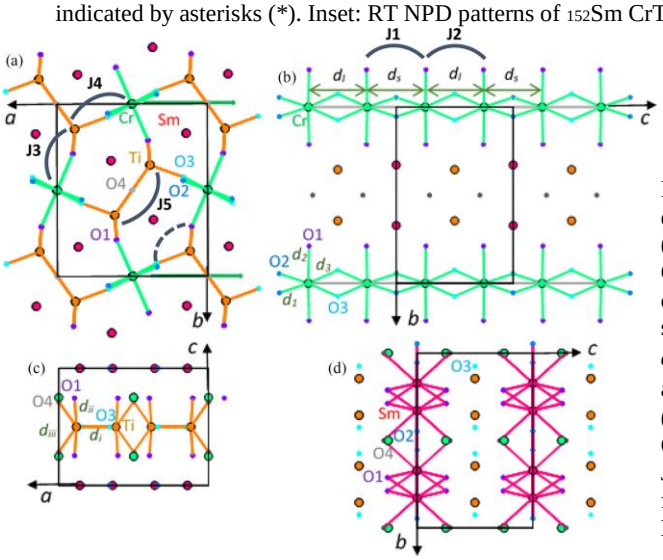

FIG. 2. Drawings of the structure: (a) Projection along *c*; the labels of the elements are indicated and the Cr–O and Ti–O bonds are shown. (b) Projection along *a*; the Cr-O distances are drawn to highlight the chains of CrO_6 octahedra running along *c*; the correspondence of the chains between (a) and (b) panels is indicated by horizontal green arrows; short and long Cr-Cr distances are labeled d_s and d_l, respectively; and d_1, d_2, and d_3 correspond to Cr-O distances with $d_1 < d_2 < d_3$. (c) Projection along *b*: only Ti–O bonds are shown with labels $d_i < d_{ii} < d_{iii}$; (d) *bc* plane as (b) but with the Sm–O bonds. In (a), the dotted arc shows the Cr-O-(Ti)-O-Cr supersuperexchange coupling; the J3, J4, and J5 arcs indicate the magnetic inter chain pathways, and J1, J2 arcs in (b) are for the coupling along the chain, following notation used for $NdMn_2O_5$ [9].

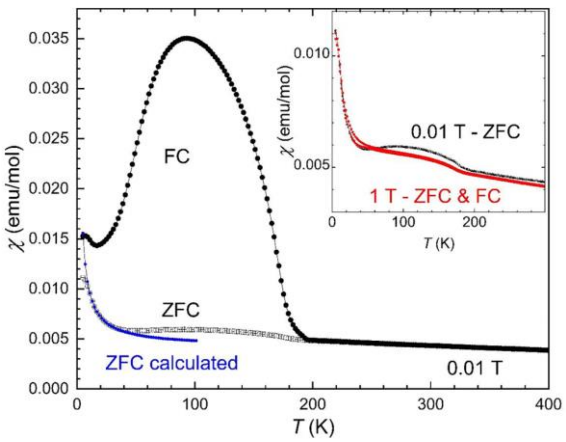

FIG. 3. Magnetic susceptibility curves recorded during heating in ZFC and FC modes (0.01 T); the blue curve is calculated using the $\chi_{Sm} = 4.22 \times 10^{-3} + 0.0608/(T + 0.37)$ formula (as discussed in Sec. IIIB). Inset: ZFC curve in 0.01 T and ZFC and FC curves in 1 T.

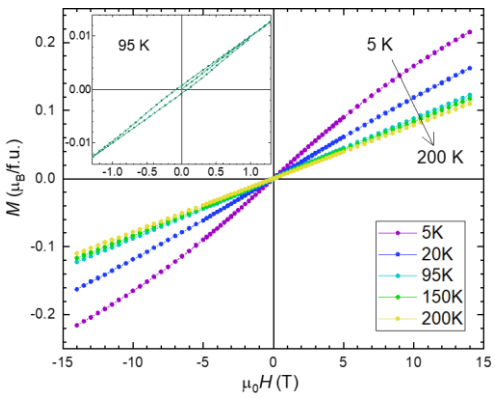

FIG. 4. Magnetization vs applied magnetic field measured at several temperatures. Detail of the 95 K curve in inset.

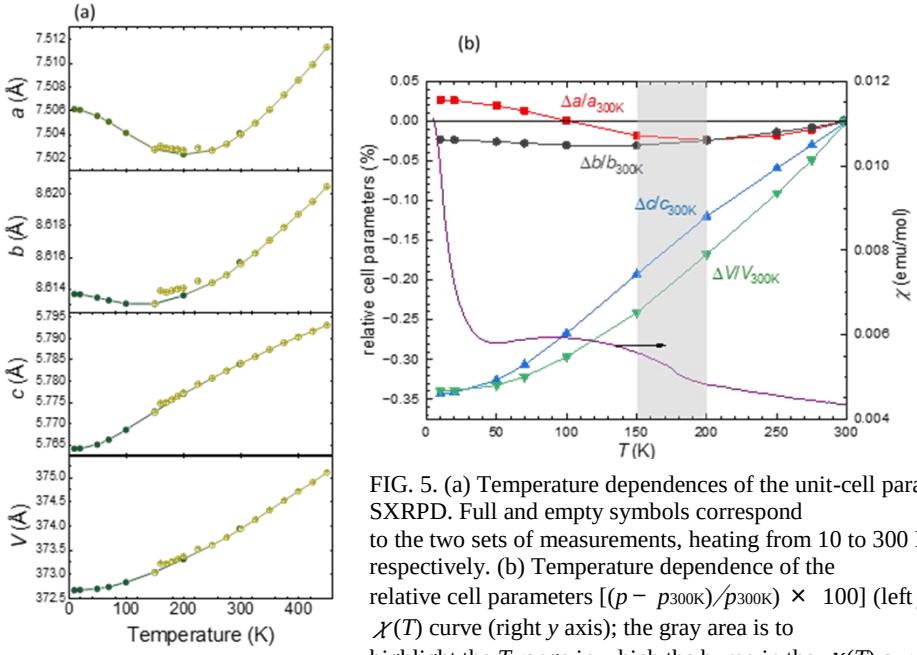

FIG. 5. (a) Temperature dependences of the unit-cell parameters of $SmCrTiO_5$ obtained from SXRPD. Full and empty symbols correspond to the two sets of measurements, heating from 10 to 300 K and cooling from 450 to 150 K, respectively. (b) Temperature dependence of the relative cell parameters $[(p - p_{300K})/p_{300K}) \times 100]$ (left *y* axis) superimposed with the ZFC $\chi(T)$ curve (right *y* axis); the gray area is to highlight the *T* range in which the bump in the $\chi(T)$ curve corresponds to the minimal value of the *a* parameter.

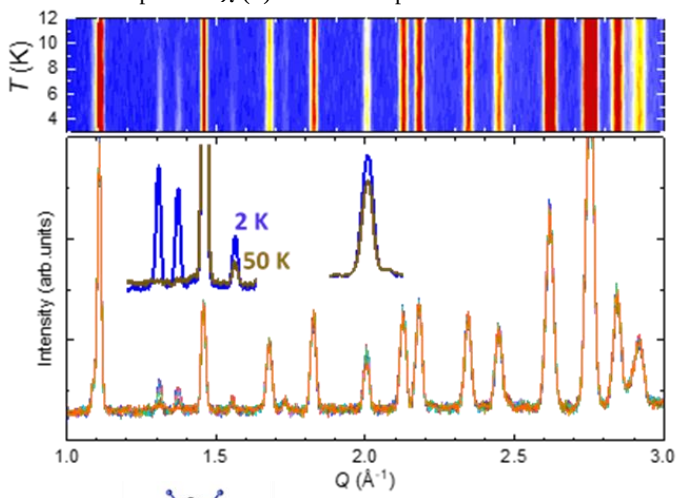

FIG. 6. Temperature evolution of neutron-diffraction patterns of ^{152}S $mCrTiO_5$ measured on the D1B diffractometer. Only the small angle region is presented, temperature ranging from 3 K (pink) to 12 K (orange), to show the magnetic contribution to neutron scattering.
The appearance of magnetic peaks at temperatures below 12 K is clearly visible in the top panel. Selected *Q* areas, centered around 1.5 and 2 $Å^{-1}$, of 2 and 50 K patterns are also shown to highlight the magnetic contribution.

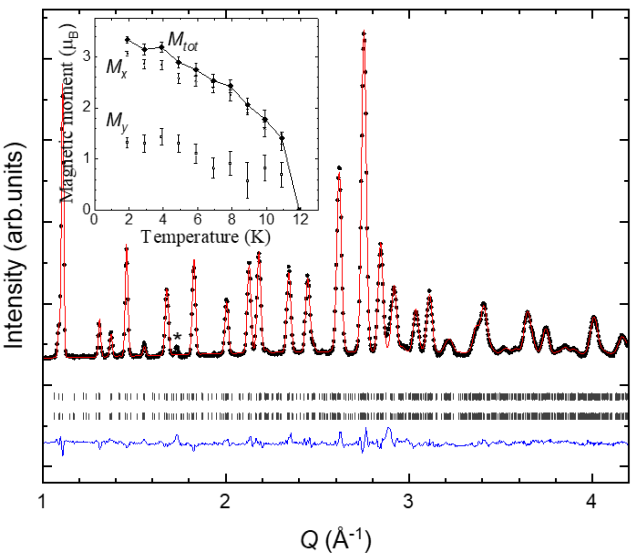

FIG. 8. Rietveld refinement of D1B NPD data of ^{152}S $mCrTiO_5$ recorded at 2 K. Observed data (black dots), calculated model (red line), and difference (blue solid line) are shown over the entire *Q* range. Ticks indicate the Bragg reflections of nuclear (top) and magnetic structure (bottom). The * indicates the main peak of Cr_2O_3 observed as impurity (≈3. 3% in mass). The temperature dependence of the magnetic moment of Cr^{3+}, obtained from Rietveld refinement using neutron-diffraction patterns presented in Fig. 6, is plotted in Inset.

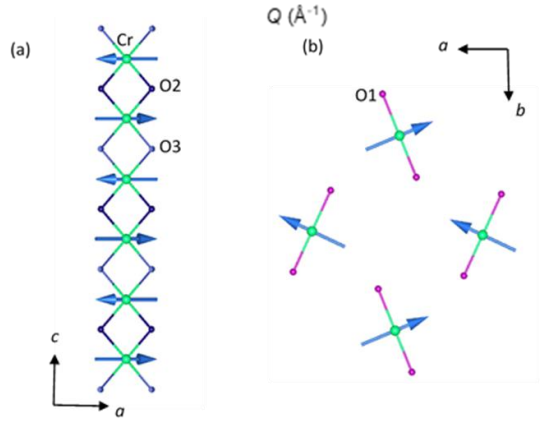

FIG. 9. Magnetic structure of $SmCrTiO_5$ at 2 K. The arrows indicate the directions of the magnetic moments of chromium ions (green circles) in the crystallographic position 4 *f* (0 0.5 *z*), i.e., located in the oxygen octahedra: (a) projection along *b* to show a CrO_6 file running along the *c* axis, and (b) projection along *c* for a two-dimensional representation of one *ab* plane [orientation as Fig. 2(a)]; two successive planes are AF coupled.

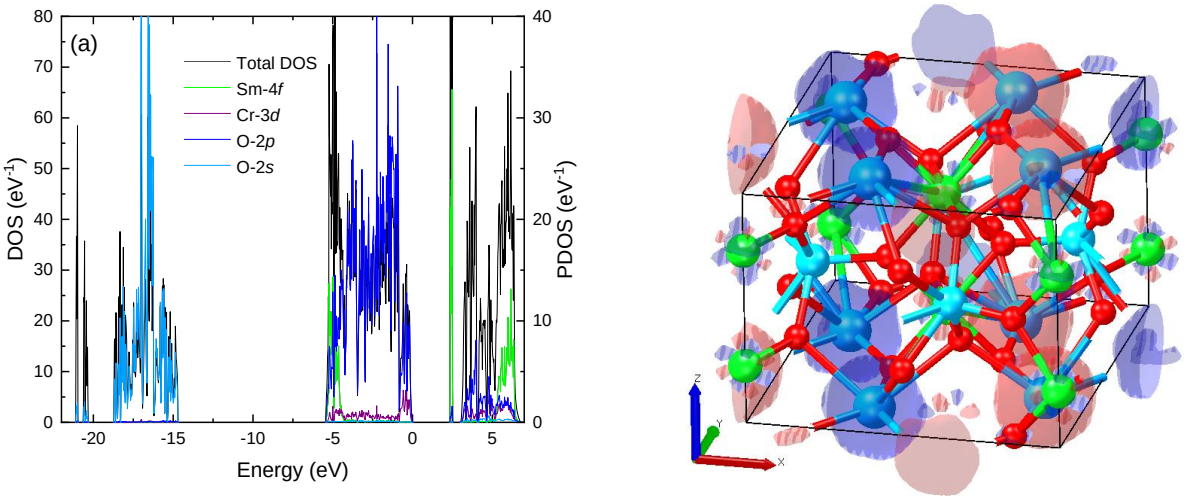

FIG. 7. (a) Total and partial (atom and orbital-projected) valence-electron density of states (DOS and PDOS) of $SmCrTiO_5$ calculated as a function of energy with respect to Fermi level (E_F = 0 eV, set to VBM). (b) Magnetization density (0.03 and −0.03 e/$Å^3$ isosurfaces depicted in blue and red, respectively) along the *x* direction calculated for the *x* magnetic quantization axis.